European Polymer Journal 45 (2009) 284–294

Contents lists available at ScienceDirect

European Polymer Journal

journal homepage: www.elsevier.com/locate/europolj

Short communication

Synthesis, photophysics and electroluminescence of new vinylene-copolymers with 2,4,6-triphenylpyridine kinked segments along the main chain

John A. Mikroyannidis [a,*], Panagiotis A. Damouras [a], Vasilis G. Maragos [a], Lin-Ren Tsai [b], Yun Chen [b,*]

[a] Chemical Technology Laboratory, Department of Chemistry, University of Patras, GR-26500 Patras, Greece
[b] Department of Chemical Engineering, National Cheng Kung University, Tainan, 701, Taiwan

ARTICLE INFO

Article history:
Received 6 July 2008
Received in revised form 10 October 2008
Accepted 10 October 2008
Available online 22 October 2008

Keywords:
Heck coupling
Pyridine
Fluorene
Carbazole
Kinked structures
Light-emitting diodes (LEDs)

ABSTRACT

Two new vinylene alternating copolymers **F** and **C** that contained 2,4,6-triphenylpyridine as a common moiety and fluorene or carbazole, respectively, as an alternating moiety were prepared by Heck coupling. They showed an outstanding thermal stability being stable up to approximately 350 °C and had relatively high glass transition temperatures (140 and 111 °C). The existence of the 2,4,6-triphenylpyridine kinked units along the polymer backbone caused a partial interruption of the π-conjugation. The copolymers emitted blue-green light with emission maximum at 446–464 nm and quantum yields of 0.52 and 0.28 in THF solution. The electrochemical properties of copolymers **F** and **C**, including HOMO and LUMO levels, were estimated from their cyclic voltammograms. Their electroluminescence (EL) emission maxima (greater than 500 nm) showed significant red-shifts relative to the PL maxima, which has been explained by the direct cross recombination transition between electrons and holes trapped on carbazole or triphenylpyridine subunits. Moreover, the emission colors transform gradually with increasing bias and approach to white color at about 30 ~ 35 V. The maximal luminance (maximal luminance efficiency) of the EL devices (ITO/PEDOT:PSS/**F** or **C**/Ca/Al) were 647 cd/m^2 (0.13 cd/A) or 615 cd/m^2 (0.10 cd/A), respectively.

1. Introduction

Conjugated polymers have been incorporated as active materials into several kinds of electronic devices such as transistors [1] and light-emitting diodes [2] (LEDs), including flexible displays [3]. Among the electroluminescent (EL) conjugated polymers poly(*p*-phenylenevinylene)s (PPVs) and poly(9,9-dialkylfluorenes) (PFs) have attracted the most general interest. Many different PPV derivatives have been synthesized in a number of ways [4]. Most of these polymers have low electron affinity. Conjugated polymers with high electron affinity are desired for certain applications, for example in LEDs. High electron affinity allows the fabrication of LEDs with good electron injection from stable cathodes like aluminum rather than the low work function metals required for more electron-rich polymers [5].

One way to achieve high electron affinity is to attach electron-withdrawing groups to the polymer like, for example, the cyano groups in poly[2,5-bis(hexyloxy)-1,4-phenylene-(1-cyanovinylene)] (CN-PPV) [5]. Another way is to use electron-deficient rings like pyridine in the polymer backbone [4]. Compared to benzene, pyridine is an electron-deficient aromatic heterocycle, with a localized lone pair of electrons in an sp^2 orbital on the nitrogen atom; consequently, the derived polymers have increased

* Corresponding authors.
E-mail addresses: mikroyan@chemistry.upatras.gr (J.A. Mikroyannidis), yunchen@mail.ncku.edu.tw (Y. Chen).

0014-3057/$ - see front matter © 2008 Elsevier Ltd. All rights reserved.
doi:10.1016/j.eurpolymj.2008.10.015

electron affinity [6], improved electron-transporting properties, and the symmetry of poly(phenylene) systems is broken. The application of pyridine as the π-deficient moiety is driven by the consideration that its homopolymer (PPy) has been used in blue-emitting devices [7,8] and that other pyridine-containing copolymers have been demonstrated to be highly luminescent [9]. In addition, introduction of the pyridinyl moiety in the polymer backbone not only increases the electron affinity of the polymer, which makes the polymer more resistant to oxidation and also gives the polymer better electron-transporting properties, but also avoids fluorescence quenching due to the intersystem crossing (ISC) effect of heavy atom [10]. Certain pyridine-containing conjugated polymers have been synthesized and characterized recently [11–13]. Moreover, poly(*p*-pyridylvinylene)polymers have been extensively investigated and present the advantages of facile n-doping (high electron affinity) and of tuning their electrooptical properties by coordination of different guests to the lone pair of nitrogen atoms [14–20].

The introduction of disorder to a conjugated system such as PF is one of the common approaches to suppress the long wavelength emissions, for example, 3,6-carbazole [21], quinoxaline or *N*,*N*′-diphenyl-*N*,*N*′-bis(4-phenyl)-1,1-biphenyl-4,4′-diamine (TPD) [22,23]. Moreover, the introduction of such a "kink" disorder on the conjugated polymer chain can efficiently depress the aggregation phenomena and its effect on the excimer formation. Poly(phenylene vinylene) derivative containing kinked 2,6-diphenylpyridine and 2,5-didodecyloxy-1,4-divinylbenzene repeat units was prepared and it was a green-yellowish emitting material [20,24].

In this investigation we describe the synthesis, characterization, photophysics, the redox and electroluminescent properties of two new vinylene alternating copolymers. They were successfully prepared by Heck coupling and contained the kinked 2,4,6-triphenylpyridine as a common moiety and fluorene or carbazole as alternating moiety. The alkyl side groups, which are attached to the fluorene or carbazole units, enhance the copolymer solubility. The existence of the pyridine units along the main chain is expected to improve the electron-transporting properties of the polymers. The introduction of carbazole units may also influence the HOMO energy level resulting in better hole-transporting ability for the polymer.

2. Experimental

2.1. Characterization methods

IR spectra were recorded on a Perkin-Elmer 16PC FT-IR spectrometer with KBr pellets. ^{1}H NMR (400 MHz) spectra were obtained using a Brucker spectrometer. Chemical shifts (δ values) are given in parts per million with tetramethylsilane as an internal standard. UV–vis spectra were recorded on a Beckman DU-640 spectrometer with spectrograde THF. The PL spectra were obtained with a Perkin-Elmer LS45 luminescence spectrometer. The PL spectra were recorded with the corresponding excitation maximum as the excitation wavelength. TGA was performed on a DuPont 990 thermal analyzer system. Ground samples of about 10 mg each were examined by TGA and the weight loss comparisons were made between comparable specimens.

Dynamic TGA measurements were made at a heating rate of 20 °C /min in atmospheres of N_2 at a flow rate of 60 cm^3/min. Thermomechanical analysis (TMA) was recorded on a DuPont 943 TMA using a loaded penetration probe at a scan rate of 20 °C/min in N_2 with a flow rate of 60 cm^3/min. The TMA experiments were conducted at least in duplicate to ensure the accuracy of the results. The TMA specimens were pellets of 10 mm diameter and ~1 mm thickness prepared by pressing powder of sample for 3 min under 8 kp/cm^2 at ambient temperature. The T_g is assigned by the first inflection point in the TMA curve and it was obtained from the onset temperature of this transition during the second heating. Elemental analyses were carried out with a Carlo Erba model EA1108 analyzer.

To measure the PL quantum yields (Φ_f) degassed solutions of the copolymers in THF were prepared. The concentration was adjusted so that the absorbance of the solution would be lower than 0.1. The excitation was performed at the corresponding excitation maximum and a solution in 1 M H_2SO_4 of quinine sulfate, which has Φ_f of 0.546 was used as a standard.

The oxidation and reduction properties of the polymers were measured with a cyclic voltammeter (model CV-50 W from BAS) under nitrogen atmosphere using a cyclic voltammetric potential excitation. The measuring cell comprised a glassy carbon coated with polymers (**F** or **C**) as the working electrode, an Ag/AgCl electrode as the reference electrode, and a platinum wire electrode as the auxiliary electrode, supporting in 0.1 M (n-Bu)$_4$NClO$_4$ in acetonitrile. The scan rate was 100 mV/s. The energy levels were calculated using the ferrocene (FOC) value of −4.8 eV with respect to vacuum level, which is defined as zero [25].

Double-layer EL devices with a configuration of ITO/PEDOT:PSS/**F** or **C**/Ca/Al were fabricated by successive spin-coating of poly(3,4-ethylenedioxythiophene) (PEDOT:PSS: Baytron P from Bayer) as hole-injection layer and **F** or **C** (30 mg/mL in chlorobenzene) as emissive layer onto ITO glass. Finally, calcium and aluminum was deposited as cathode via vacuum evaporation under 1.8×10^{-6} Torr. The devices were fabricated in the ambient conditions and then their optoelectronic properties tested in a glove box filled with nitrogen. Device performance and electroluminescence spectra were investigated and recorded, respectively, using a combination of Keithley power supply (model 2400) and Ocean Optics usb2000 fluorescence spectrophotometer.

2.2. Reagents and solvents

N,*N*-Dimethylformamide (DMF) was dried by distillation over CaH_2. Triethylamine was purified by distillation over KOH. All other reagents and solvents were commercially purchased and were used as supplied.

2.3. Preparation of starting materials

2.3.1. 2,6-Bis(4-bromophenyl)-4-phenylpyridine (1)

The preparation and characterization of this compound has been described in our previous publication [20].

2.3.2. 9,9-Dihexyl-2,7-divinylfluorene (2)

This compound was prepared by Stille coupling reaction [26] of 2,7-dibromo-9,9-dihexylfluorene with tributylvinyltin in the presence of $PdCl_2(PPh_3)_2$ as catalyst and a few crystals of 2,6-di-*tert*-butylphenol as polymerization inhibitor utilizing toluene as reaction medium. The synthesis and characterization of **2** has been described in our previous publication [27].

2.3.3. 9-Hexyl-3,6-divinylcarbazole (3)

This compound was similarly prepared by Stille coupling reaction [26] of 9-hexyl-3,6-dibromocarbazole with tributylvinyltin. The spectroscopic characterization of this compound conforms to literature [28].

2.4. Preparation of copolymers

The preparation of **F** is given as a typical example for the preparation of copolymers. A flask was charged with a mixture of **1** (0.2678 g, 0.576 mmol), **2** (0.2226 g, 0.576 mmol), $Pd(OAc)_2$ (0.0054 g, 0.024 mmol), P(*o*-tolyl)$_3$ (0.0403 g, 0.132 mmol), DMF (5 mL) and triethylamine (2 mL). The flask was degassed and purged with N_2. The mixture was heated at 90 °C for 24 h under N_2. Then, it was filtered and the filtrate was poured into methanol. The yellow precipitate was filtered and washed with methanol. The crude product was purified by dissolving in THF and precipitating into methanol (0.2879 g, 72%).

FT-IR (KBr, cm^{-1}) (Fig. 1a): 3024, 2924, 2854, 1700, 1594, 1542, 1490, 1464, 1416, 1392, 1008, 960, 826, 760, 696.

^{1}H NMR ($CDCl_3$, ppm) (Fig. 2a): 8.26 (m, 4H, aromatic h); 7.93 (m, 2H, aromatic e); 7.85–7.77 (m, 4H, aromatic d); 7.72 (m, 6H, aromatic g); 7.55 (m, 5H, aromatic i); 7.32–7.27 (m, 4H, olefinic f); 2.05 (m, 4H, aliphatic c); 1.09 (m, 16H, aliphatic b); 0.77 (t, 6H, aliphatic a).

Anal. Calcd. for $(C_{52}H_{51}N)_n$: C, 90.52; H, 7.45; N, 2.03. Found: C, 89.87; H, 7.52; N, 2.11.

Copolymer **C** was similarly prepared as a yellow solid in 66% yield from the reaction of **1** with **3**.

FT-IR (KBr, cm^{-1}) (Fig. 1b): 3026, 2924, 2856, 1706, 1596, 1542, 1486, 1450, 1390, 1238, 1182, 960, 824, 762, 696.

^{1}H NMR ($CDCl_3$, ppm) (Fig. 2b): 8.23 (m, 4H, aromatic h); 8.09 (m, 2H, aromatic k); 7.71 (m, 6H, aromatic g); 7.64 (m, 2H, aromatic i); 7.54 (m, 7H, aromatic e); 7.38–7.27 (m, 4H, olefinic f); 4.27 (m, 2H, aliphatic d); 1.87 (m, 2H, aliphatic c); 1.30 (m, 6H, aliphatic b); 0.88 (t, 3H, aliphatic a).

Anal. Calcd. for $(C_{45}H_{38}N_2)_n$: C, 89.07; H, 6.31; N, 4.61. Found: C, 88.53; H, 6.25; N, 4.57.

3. Results and discussion

3.1. Synthesis and characterization

The key dibromide **1** was prepared from the reaction of benzaldehyde with 4-bromoacetophenone in the presence of CH_3COONH_4/CH_3COOH. The synthesis and characterization

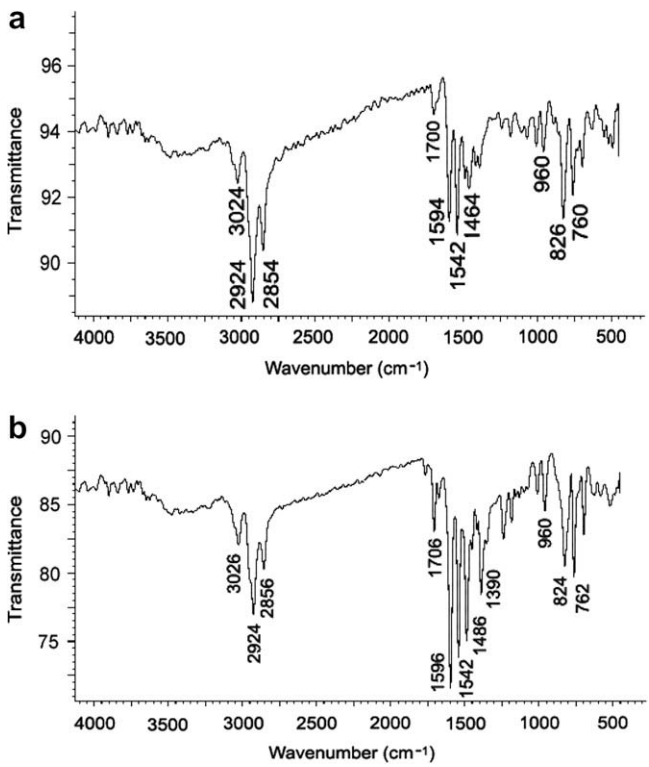

Fig. 1. FT-IR spectra of copolymers **F** (a) and **C** (b).

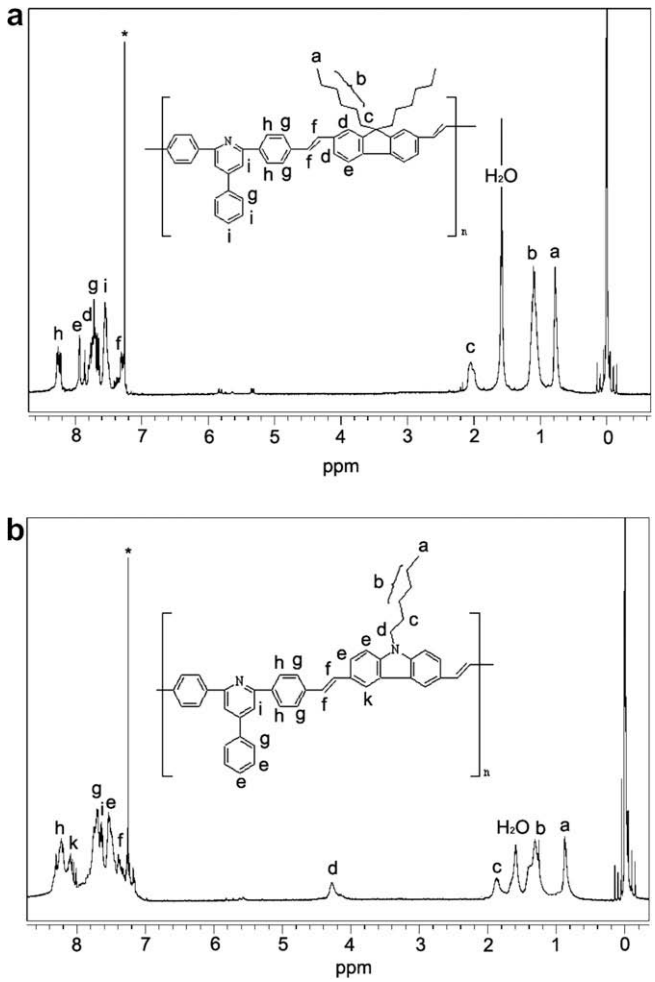

Fig. 2. ^{1}H NMR spectra in $CDCl_3$ solution of copolymers **F** (a) and **C** (b). The solvent peak is denoted by an asterisk.

of **1** has been described in our previous publication [20]. On the other hand, the two divinyls **2** and **3** were prepared from the corresponding dibromides by Stille reaction [26].

The two vinylene alternating copolymers **F** and **C** were prepared by Heck coupling of dibromide **1** with divinyls **2** and **3**, respectively (Scheme 1). These copolymers were purified by dissolving in THF and precipitating into methanol. The preparation yields for **F** and **C** were 72 and 66%, and the number-average molecular weights (M_n) that were determined by GPC were 8500 and 10200 with polydispersity 1.7 and 2.2, respectively (Table 1).

The copolymers were very soluble in common organic solvents such as THF, chloroform, dichloromethane and toluene. They dissolved also in strong organic solvents like formic acid and trifluoroacetic acid because of the protonation of the pyridine ring.

The structural characterization of copolymers was accomplished by FT IR and ^{1}H NMR spectroscopy. The IR spectra (Fig. 1) showed certain common absorption band which for **F** appeared at 3024, 1700, 1594, 1464, 1392, 826, 760 (aromatic and pyridine ring); 2924, 2854 (C-H stretching of the aliphatic side chains) and 960 cm^{-1} (trans olefinic bond). The ^{1}H NMR spectra (Fig. 2) displayed an upfield multiplet at 8.26–8.23 ppm assigned to the protons labeled "h" which are deshielded from the pyridine ring. **C** exhibited also an upfield signal at 8.09 ppm assigned to the carbazole proton labeled "k". Generally, the aromatic protons resonated at the region of 8.26–7.54 ppm, while the aliphatic protons of the side chains resonated at 4.27–0.77 ppm. The olefinic protons resonated at 7.38–7.27 ppm and they were partially overlapped with the chloroform peak. Finally, all ^{1}H NMR spectra showed small signals between 5 and 6 ppm from the protons CH_2=CH– of the vinyl end groups. The peak at ~1.60 ppm which appears in the ^{1}H NMR spectra of both copolymers is associated with the water. Since the spectra of **F** and **C** have been recorded using different solution concentrations of the copolymers and different spectrum amplitudes, the intensity of the water signal could not be correlated with the hydrophilicity of the copolymers.

TGA and TMA were used for thermal characterization of copolymers (Fig. 3, Table 1). The copolymers showed an excellent thermal stability since they were stable up to approximately 350 °C. The decomposition temperature

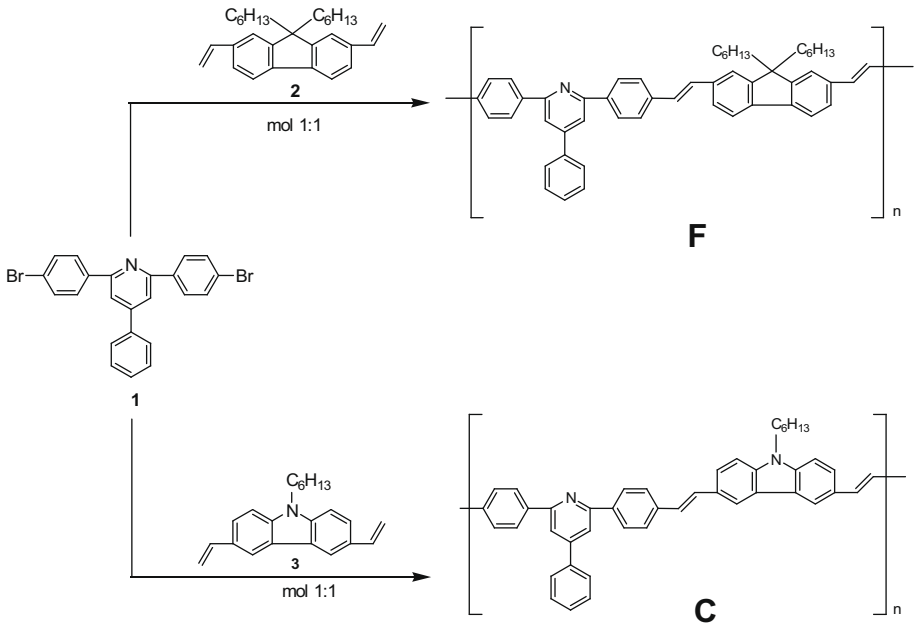

Scheme 1. Synthesis of copolymers **F** and **C**.

Table 1
Molecular weights and thermal characteristics of copolymers.

Copolymer	M_n[a]	M_w/M_n[a]	T_d[b] (°C)	Y_c[c] (%)	T_g[d] (°C)
F	8500	1.7	419	56	140
C	10200	2.2	412	66	111

[a] Molecular weights determined by GPC using polystyrene standards.
[b] Decomposition temperature corresponding to 5% weight loss in N_2 determined by TGA.
[c] Char yield at 800 °C in N_2, determined by TGA.
[d] Glass transition temperature determined by TMA.

(T_d) was 412–419 °C while the char yield (Y_c) was 56–66% at 800 °C in N_2. **F** displayed higher rigidity than **C** since the glass transition temperature (T_g) was 140 and 111 °C, respectively. The different number of hexyl side groups per repeat unit of the polymers and the different nature of the substituted 2,7-fluorene and 3,6-carbazole rings are expected to affect the T_g values. The T_g value was determined from the onset temperature of the TMA transition that was recorded during the second heating when a penetration probe was used (insert of Fig. 3). The relatively high T_d and T_g values of the present polymers bodes well, because the lifetime of the polymer LEDs is depended on their thermal stability.

3.2. Photophysical properties

Figs. 4 and 5 present the normalized UV–vis absorption spectra and the photoluminescence (PL) emission spectra of copolymers in both dilute (10^{-5} M) THF solution and thin film. Table 2 summarizes the photophysical characteristics of copolymers.

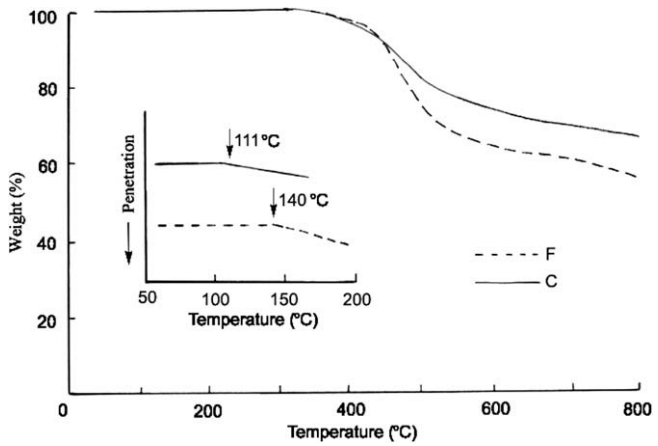

Fig. 3. TGA thermograms of copolymers in N_2. The insert shows the TMA traces of copolymers. Conditions: N_2 flow, 60 cm^3/min; heating rate, 20 °C/min.

The absorption spectra (Fig. 4) showed an absorption maximum ($\lambda_{a,max}$) at 357–396 nm corresponding to the π-$\pi*$ transition of the polymer backbone. The absorption curve of **C** was more broad than that of **F** in solution and thin film and had the most blue-shifted $\lambda_{a,max.}$ However, the optical band gaps (E_g^{opt}) of the polymers, that were determined from their absorption onset in thin film, were almost identical ($\sim$ 2.76 eV). These E_g^{opt} are comparable to that of poly(9,9-dioctylfluorene-2,7-vinylene) [29] (2.6 eV) and higher than that of poly(1-methoxy-4-(2-ethyl-hexyloxy)-*p*-phenylenevinylene) (MEH-PPV) [30] (2.21 eV).

The emission spectra of copolymers (Fig. 5) were similar with emission maximum ($\lambda_{f,max}$) at 446–452 nm in solution and 460–464 nm in thin film. This indicates that the chemical structure of the second moiety of the repeating unit, namely the divinylenefluorene and divinylenecarbazole, did not influence significantly their emission. A red-shift by 8–18 nm of the $\lambda_{f,max}$ was observed upon going from solution to thin film due to the formation of aggregates in solid state. Generally, the π-conjugation along the backbone of these polymers was disrupted by the kinked structure of the 2,4,6-triphenylpyridine. Thus these polymers emitted blue-green light on photoexcitation, while the alkoxy-substituted poly(*p*-phenylenevinylene)s (PPVs) emitted at the green-yellow region (520–51 nm) [20].

The PL efficiency of the copolymers in solution was evaluated by determination [31] of their quantum yields (Φ_f's) relative to quinine sulfate (Table 2). **F** was much higher photoluminescent than **C** since had $\Phi_f = 0.52$ while **C** had $\Phi_f = 0.28$.

3.3. Electrochemical properties

Homogeneous films were readily obtained for both copolymers **F** and **C** by spin-coating from their solution in chlorobenzene. This is owing to their moderate high molecular weight and good solubility in chlorobenzene. Therefore, electrochemical properties of the **F** and **C** were investigated using the films formed directly on the electrode surface. Cyclic voltammetry (CV) was performed upon the electrode immersed in an electrolyte of 0.1 M $(n\text{-Bu})_4NClO_4$ in acetonitrile.

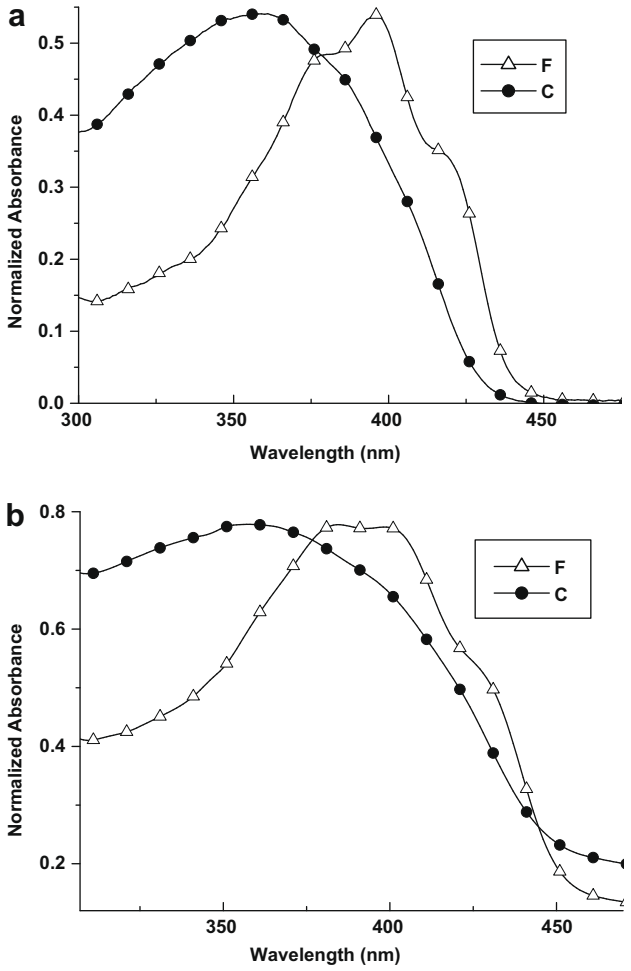

Fig. 4. Normalized UV–vis absorption spectra of copolymers in 10^{-5} M THF solution (a) and thin film (b).

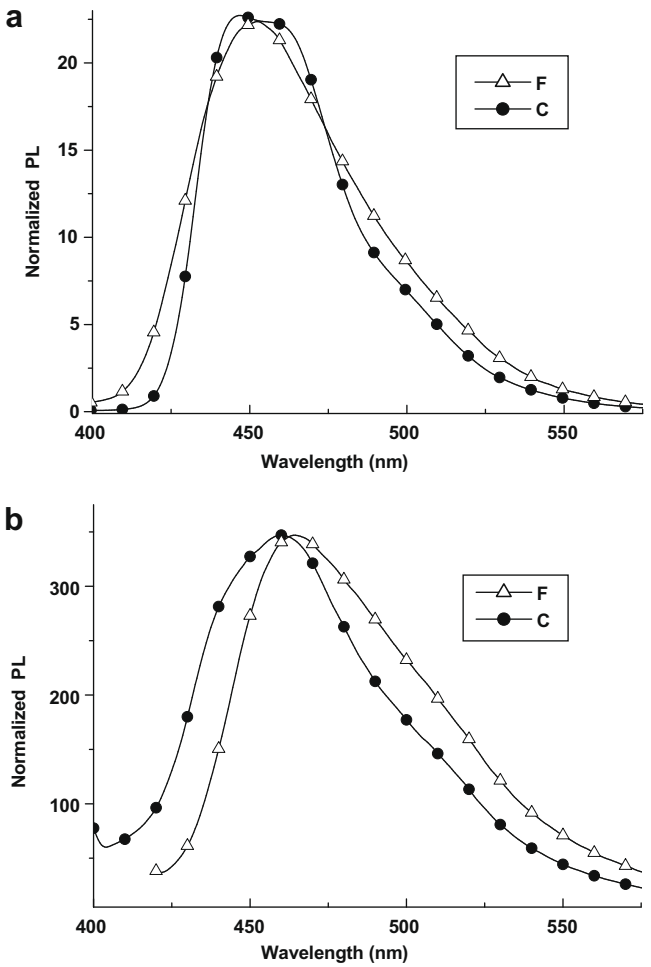

Fig. 5. Normalized PL emission spectra of copolymers in 10^{-5} M THF solution (a) and thin film (b). The PL emission spectra were recorded using as excitation wavelength the corresponding excitation maximum.

As shown in Fig. 6, during the anodic scan the oxidation starts at 0.60 and 0.37 V (versus FOC) for the **F** and **C** films, respectively. The electrochemical data are summarized in Table 3. Lower onset oxidation potential of **C** is due to its repeating carbazole segments, which has been well known as an electron donor. However, during the cathodic scan, the reduction begins at -2.00 V and −2.12 V (versus FOC) for the **F** and **C** films respectively. Thus copolymer **C** is more difficult to be reduced than polymer **F** due also to the carbazole repeating units in the main chain. The HOMO and LUMO energy levels of **F**, estimated by comparing with −4.8 eV of ferrocene (FOC), are −5.40 eV and −2.80 eV, respectively, from which the electrochemically-estimated band gap (E_g^{el}) is 2.60 eV. By similar methods, the HOMO and LUMO levels of **C** are calculated to be −5.17 eV and −2.68 eV with a band gap of 2.49 eV. Clearly, both HOMO and LUMO levels are raised when the fluorene moiety in **F** (−5.40 eV, −2.80 eV) is replaced by the carbazole unit (**C**: −5.17 eV, −2.68 eV). This is mainly owing to that the carbazole unit is much more electron-donating than the

Table 2
Photophysical properties of copolymers.

Copolymer	$\lambda_{a,max}$[a] in THF solution (nm)	$\lambda_{f,max}$[b] in THF solution (nm)	Φ_f[c] in THF solution	$\lambda_{a,max}$[a] in thin film (nm)	$\lambda_{f,max}$[b] in thin film (nm)	$E_g$opt (eV)[d]
F	396	446	0.52	385	464	2.76
C	361	452	0.28	357	460	2.77

[a] $\lambda_{a,max}$, The absorption maxima from the UV–vis spectra in 10^{-5} M THF solution or in thin film.
[b] $\lambda_{f,max}$, The PL emission maxima in 10^{-5} M THF solution or in thin film.
[c] Φ_f, PL quantum yield.
[d] E_g^{opt}, The optical band gap calculated from the onset of thin film absorption spectrum. The PL emission spectra were recorded using as excitation wavelength the corresponding excitation maximum.

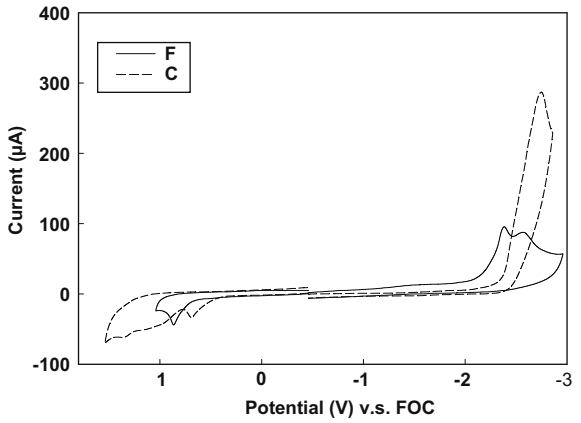

Fig. 6. Cyclic voltammograms of copolymers **F** and **C**; scan rate: 100 mV/s.

fluorene group. The higher LUMO level in **C** will reduce the electron injection ability, while the hole injection ability will be enhanced. As mentioned above, the optically-derived band gap (E_g^{opt} in Table 2) estimated from onset absorption is *ca.* 2.76 eV for both **F** and **C**, which is greater than those obtained from electrochemical data. This can be attributed to that oxidation and reduction might start from different portions of the copolymers composed of 2,4,6-triphenylpyridine and 2,7-divinylfluorene or 3,6-divinylcarbazole subunits. Especially for polymer **C** the oxidation and reduction might begin from the 3,6-divinylcarbazole and 2,4,6-triphenylpyridine moieties, respectively. This usually leads to reduced band gap (E_g^{el}) when compared with that estimated from onset absorption (E_g^{opt}) [32]. Accordingly, the oxidation and reduction under a bias will start from 3,6-divinylcarbazole and 2,4,6-triphenylpyridine subunits, respectively. The electrochemically-obtained band gap is the energy difference between LUMO level of 2,4,6-triphenylpyridine units and HOMO level of 3,6-divinylcarbazole units. However, the optically-estimated band gap is the energy difference between LUMO and HOMO levels of the longer wavelength emitting segments.

Table 3
Electrochemical data of **F** and **C**.

Copolymer	$E_{onset(red)}$[a] (V) *vs.* FOC	$E_{onset(ox)}$[a] (V) *vs.* FOC	E_{LUMO}[b] (eV)	E_{HOMO}[c] (eV)	E_g^{el} (eV)[d]
F	−2.00	0.60	−2.80	−5.40	2.60
C	−2.12	0.37	−2.68	−5.17	2.49

[a] E_{FOC} = 0.48 V vs. Ag/AgCl.
[b] $E_{LUMO} = -e(E_{onset(red),\ FOC} + 4.8\ V)$.
[c] $E_{HOMO} = -e(E_{onset(ox),\ FOC} + 4.8\ V)$.
[d] Band gaps estimated from electrochemical data: $E_g^{el} = |E_{LUMO} - E_{HOMO}|$.

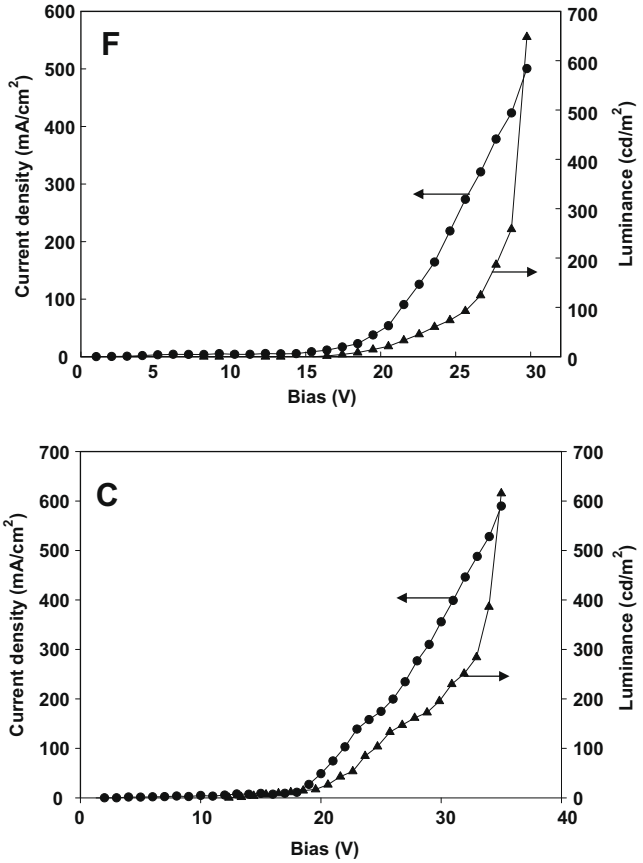

Fig. 7. Luminance-voltage (▲) and current density-voltage (●) characteristics of **F** and **C** devices; Device configuration: (ITO/PEDOT:PSS/polymer/Ca/Al).

Table 4
Electroluminescence properties of the PLEDs (ITO/PEDOT:PSS/polymer/Ca/Al).

Copolymer	Turn-on voltage (V)	L_{max}[a] (cd/m^2)	LE[b] (cd/A)	Bias (V)	Current density[c] (mA/cm^2)	CIE coordinates[c] (x, y)
F	16.4	647	0.13	29.7	501	(0.33, 0.38)
C	17.5	615	0.10	35.0	589	(0.34, 0.38)

[a] L_{max}, maximal luminance.
[b] LE, maximal luminance efficiency.
[c] The values at maximal luminance.

3.4. Electroluminescence properties

Two-layer EL devices with a configuration of ITO/PEDOT:PSS/**F** or **C**/Ca/Al were fabricated to investigate their optoelectronic performance. Fig. 7 shows current density-bias (*I–V*) and luminance-bias (*L–V*) characteristics of the EL devices using **F** or **C** as emitting layer. Their corresponding electroluminescence properties are summarized in Table 4. The turn-on voltages, which is defined arbitrarily as the voltages required for the luminance of 1 cd/m^2, are about 16∼17 V. The maximal luminance is 647 cd/m^2 (at 501 mA/cm^2) and 615 cd/m^2 (at 589 mA/cm^2) for **F** and **C** devices, respectively. Their maximal luminance efficiencies are also comparable and reveal values at 0.10∼0.13 cd/A. The introduction of 2,4,6-triphenylpyridine into **F** and **C** should increase their electron affinity. For instance, the LUMO level of **F** (−2.80 eV) is lower than that of PC (−2.77 eV) containing 2,4,6-triphenylbenzene groups reported previously [20,24], although the PC possesses two additional dodecyloxy groups in each repeating unit. Lower LUMO level usually leads to enhanced electron affinity. However, the LUMO level of **C** (−2.68 eV) is higher than PC, which is probably due to the presence of strong electron-donating carbazole units.

The EL spectra of **F** and **C** devices (Fig. 8) show significant red-shift as compared with their PL spectra in film state (Fig. 5b). In addition the emission bands are very broad with the FWHM (full width at half maximum) greater than 150 nm. The abnormal EL spectra can be explained by the direct cross recombination transition between electrons and holes trapped on carbazole or triphenylpyridine subunits [33]. Such pair of trapped carriers is considered as a particular excited state (electromer) responsible also for the EL emission of some other compounds. The alternating structures of 2,4,6-triphenylpyridine with hole transporting fluorene and carbazole in copolymers **F** and **C**, respectively, contributes to the formation of the electromers. Since the holes are mainly trapped at fluorene or carbazole moieties, while the electrons are trapped at 2,4,6-triphenylpyridine units. Due to their alternate structures the trapped carriers can be proximity to each other, which leads to formation of the electromers. Moreover, it is interesting to note that the EL spectra of **C** device show obvious blue-shift (from 610 nm to 510 nm) with an increase in applied voltage from 23.7 V to 35 V. The device **F** exhibits similar blue-shift, although at a lesser extent. This color variation upon increasing bias can be more clearly observed as shown in the CIE chromaticity diagrams (Fig. 9). The emission color of the **F** device changes linearly from yellow-orange [CIE (0.38, 0.43)] to near white [CIE (0.33, 0.38)] as the operating bias increased from 21.5 to 29.7 V. However, for **C** device the color changes nonlinearly from red-orange [CIE (0.51, 0.39)] to near white [CIE (0.34, 0.38)] when the bias is increased from 21.6 V to 35 V. The blue-shift in EL emission upon increasing bias is probably due to reduced concentration of the trapped carriers (electromers) under high electrical field. It has been attributed to local heat developed under the application of electric field leading to changes in structural conformations of the chains and hence to variations in the electronic band structure [34], which in turn reduce the concentration of the electromers.

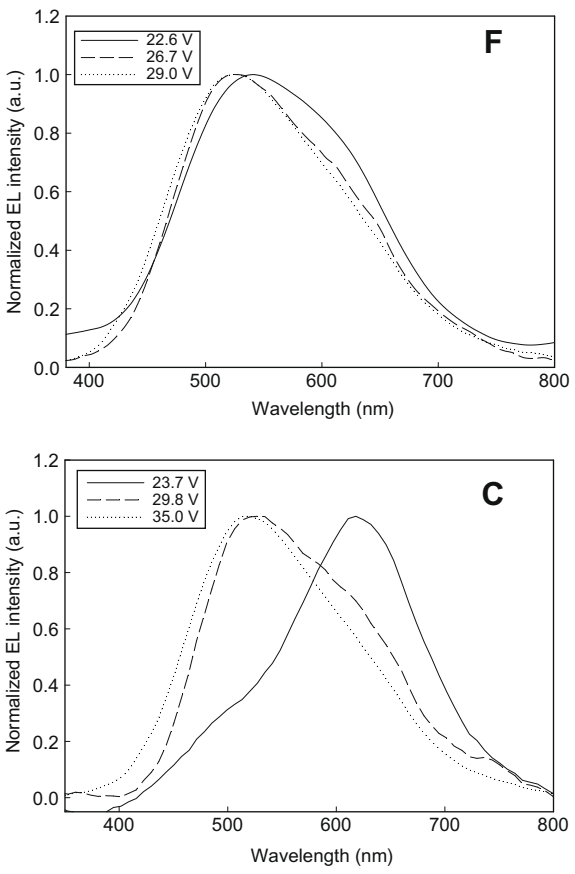

Fig. 8. Electroluminescence spectra of **F** and **C** devices under different applied voltages; Device configuration: (ITO/PEDOT:PSS/polymer/Ca/Al).

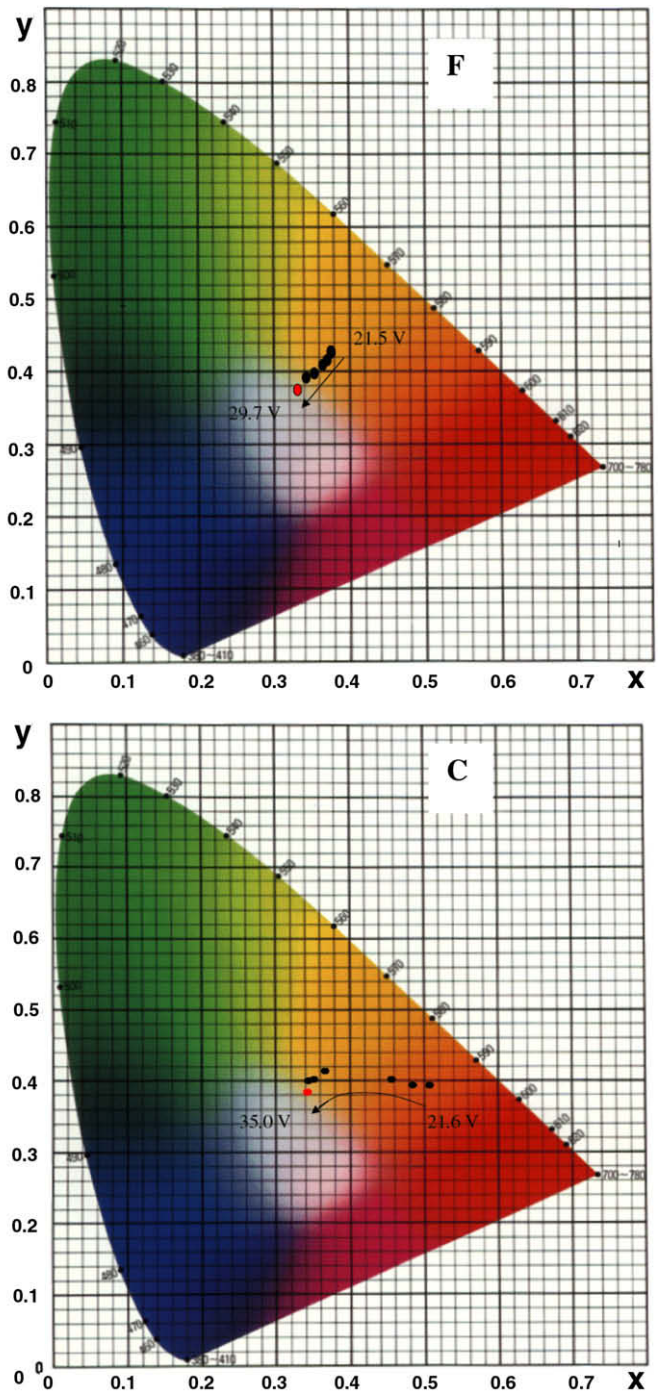

Fig. 9. Variation of CIE coordinates with increasing bias: the arrow represents the voltage increase. The red point represents the CIE (x, y) at maximal luminance.

4. Summary

The Heck coupling of 2,6-bis(4-bromophenyl)-4-phenylpyridine with divinyls afforded two new soluble vinylene alternating copolymers **F** and **C** that contained fluorene and carbazole, respectively, units. They were stable up to about 350 °C and showed relatively high glass transition temperatures of 140 and 111 °C. Both copolymers emitted blue-green light with emission maximum at 446–464 nm and quantum yields of 0.52 and 0.28 in solution. The HOMO (LUMO) levels of **F** and **C** were −5.40 eV (−2.80 eV) and −5.17 eV (−2.68 eV), respectively, from which the band gaps were estimated to be 2.60 and 2.49 eV. The maximal luminance (maximal luminance efficiency) the **F** and **C**

devices (ITO/PEDOT:PSS/polymer/Ca/Al) were 647 cd/m^2 (0.13 cd/A) and 615 cd/m^2 (0.10 cd/A), respectively. Interestingly, the emission colors of both **F** and **C** devices changed gradually from yellow-orange and red-orange, respectively, to near white with increasing operating voltages.

References

[1] Burroughes JH, Jones CA, Friend RH. Nature (London) 1988;335:137.
[2] Burroughes JH, Bradley DDC, Brown AR, Marks RN, Mackay K, Friend RH, Burns PL, Holmes AB. Nature (London) 1990;347:539.
[3] Gustafsson G, Cao Y, Treacy GM, Klavetter F, Colaneri N, Heeeger AJ. Nature (London) 1992;357:477.
[4] Kraft A, Grimsdale AC, Holmes AB. Angew Chem, Int Ed 1998;37:402–444.
[5] Greenham NC, Moratti SC, Bradley DDC, Friend RH, Holmes AB. Nature 1993:365.
[6] Kanbara T, Saito N, Yamamoto T, Kubota K. Macromolecules 1991;24:5883.
[7] Yamamoto T, Suganuma H, Saitoh Y, Maruyama T, Inoue T. Jpn J Appl Phys 1996;35:L1142.
[8] Kanbara T, Kushida T, Saito N, Kuwajima I, Kubota K, Yamamoto T. Chem Lett 1992:583.
[9] Wang YZ, Gebler DD, Fu DK, Swager TM, MacDiarmid AG, Epstein AJ. Synth Met 1997;85:1179.
[10] Turro NJ. Modern Molecular Photochemistry Benjamin/Cummings. New York: Publ. Co.; 1978 (p. 48).
[11] Ng S-C, Lu H-F, Chan HSO, Fujii A, Laga T, Yoshino K. Macromolecules 2001;34:6895.
[12] Yasuda T, Yamamoto T. Macromolecules 2003;36:7513.
[13] Wang YZ, Sun RG, Meghdadi F, Leising G, Swager TM, Epstein AJ. Synth Met 1999;102:889.
[14] Wang B, Wasielewski MR. J Am Chem Soc 1997;119:12.
[15] Gebler DD, Wang YZ, Blatchford JW, Jessen SW, Lin LB, Gustafson TL, Wang HL, Swagen TM, MacDiarmid AG, Epstein AJ. J Appl Phys 1995;78:4264.
[16] Yamamoto T, Komarudin D, Arai M, Lee BL, Suganuma H, Asakawa N, et al. J Am Chem Soc 1998;120:2047.
[17] Barashkov NN, Olivos HJ, Ferraris JP. Synth Met 1997;90:41.
[18] Wang H, Helgerson R, Ma B, Wudl F. J Org Chem 2000;65:5862.
[19] Peng Z, Galvin ME. Chem Mater 1998;10:1785.
[20] Karastatiris P, Mikroyannidis JA, Spiliopoulos IK, Fakis M, Persephonis P. J Polym Sci Part A: Polym Chem 2004;42:2214.
[21] Xia C, Advincula RC. Macromolecules 2001;34:5854.
[22] Sun Q, Zhan X, Yang C, Liu Y, Li Y, Zhu D. Thin Solid Films 2003;440:247.
[23] Wang S, Liu YQ, Zhan XW, Yu G, Zhu DB. Synth Met 2003;137:1153.
[24] Cimrova V, Hlidkova H, Vyprachticky D, Karastatiris P, Spiliopoulos IK, Mikroyannidis JA. J Polym Sci Part B: Polym Phys 2006;44:524.
[25] Liu Y, Liu M-S, Jen AK-Y. Acta Polym 1999;50:105.
[26] McKean DR, Parrinello G, Renaldo AF, Stille JK. J Org Chem 1987;52:422.
[27] Mikroyannidis JA, Yu Y-J, Lee S-H, Jin JI. J Polym Sci Part A: Polym Chem 2006;44:4494.
[28] Morin JF, Drolet N, Tao Y, Leclerc M. Chem Mater 2004;16:4619.
[29] Jin S-H, Park H-J, Kim JY, Lee K, Lee S-P, Moon D-K, Lee H-J, Gal Y-S. Macromolecules 2002;35:7532.
[30] Santos LF, Faria RC, Gaffo L, Carvalho LM, Faria RM, Gonçalves D. Electrochimica Acta 2007;52:4299.
[31] Demas JN, Crosby GA. J Phys Chem 1971;75:991.
[32] Chen S-H, Hwang S-W, Chen Y. J Polym Sci Part A: Polym Chem 2004;42:883.
[33] (a) Giro G, Cocchi M, Kalinowski J, Di Marco P, Fattori V. Chem Phys Lett 2000;318:137;
(b) Kalinowski J, Giro G, Cocchi M, Fattori V, Di Marco P. Appl Phys Lett 2000;76:2352.
[34] Mikroyannidis JA, Spiliopoulos IK, Kasimis TS, Kulkarni AP, Jenekhe SA. Macromolecules 2003;36:9295.